RESEARCH ARTICLE

FOOD SAFETY AND HEALTH

WILEY

Enhanced magnetic relaxation switching immunoassay for chlorpyrifos based on tyramine signal amplification

Chen Zhan[1] | Long Wu[2] | Yongzhen Dong[1,3] (ORCID)

[1]College of Food Science and Technology, Huazhong Agricultural University, Wuhan, Hubei, China

[2]School of Food Science and Engineering, Key Laboratory of Tropical and Vegetables Quality and Safety for State Market Regulation, Hainan University, Haikou, China

[3]Academy of Food Interdisciplinary Science, School of Food Science and Technology, Dalian Polytechnic University, Dalian, Liaoning, China

Correspondence
Yongzhen Dong and Long Wu.
Email: dongyz@dlpu.edu.cn and longquan.good@163.com

Abstract

Chlorpyrifos, an organophosphorus pesticide, is widely used in agriculture to protect crops from insects. However, the presence of its residues in food has caused widespread concern due to the serious risks to human health. Traditional detection methods suffer from limitations, such as low sensitivity, long detection time, and complicated operations. Herein, based on the tyramine signal amplification (TSA) strategy, we developed a sensitive and rapid magnetic relaxation switching (MRS) immunosensor for the detection of chlorpyrifos. Wherein, magnetic Fe_3O_4 nanoparticles modified with tyramine (MNP_{150}-tyramine) acted as magnetic probes for magnetic relaxation signal output. In the presence of hydrogen peroxide (H_2O_2) and horseradish peroxidase (HRP), tyramine can be converted to the highly reactive intermediate that covalently binds with the nearby proteins, such as HRP and antibody, thus assembling MNPs to magnetic clusters and showing changes in transverse relaxation time (T_2) signals. Based on the "antibody–antigen" immunoreaction, chlorpyrifos could make a connection of HRP/antibody-modified MNPs and MNP_{150}-tyramine with a result of MNPs aggregation and strong T_2 signals. In this study, the TSA-MRS method showed sensitive detection of chlorpyrifos with a limit of detection of 0.54 ng/mL, a 4.5-fold enhancement in the sensitivity compared with the ELISA method, providing an alternative method for the detection of harmful substances in food samples.

KEYWORDS
chlorpyrifos, magnetic probes, magnetic relaxation switching, pesticide, transverse relaxation time, tyramine signal amplification

1 | INTRODUCTION

Pesticide refers to a class of chemical substances that protect agricultural and forestry crops from diseases, insects, and grasses or regulate plant growth, which plays an important role in increasing crop yield (Li et al., 2022; Mie et al., 2018; Pundir et al., 2019). However, the excessive or abuse of pesticides usually causes a large number of pesticide residues in food stuffs, which has been identified as one of the most concerned food safety issues (Samsidar et al., 2018; Xu et al., 2017). At present, organophosphorus pesticides are the most widely used pesticides with the prohibition of highly toxic organochlorine pesticides. As an intensively used organophosphorus pesticide, chlorpyrifos plays an important role in preventing crops from damage and increasing their yields (Dong et al., 2022). Nevertheless,

the excessive use of chlorpyrifos usually causes environmental and food safety problems (Gosset et al., 2020; Liu et al., 2019; Zhu et al., 2010). Moreover, chlorpyrifos can accumulate in the human body and cause neurological or reproductive disorders, posing a serious risk to human health (Hou et al., 2018; Samsidar et al., 2018; Zhang et al., 2021). In addition, excessive levels of chlorpyrifos may cause trading problems in the export business, which can lead to serious financial losses (Katsikantami et al., 2019; Khalid et al., 2020). Thus, it is of great practical importance to develop high-performance methods for the rapid and sensitive detection of chlorpyrifos.

Currently, the detection tools for chlorpyrifos residues mainly involve the bulk instruments-based methods and rapid detection methods (Theansun et al., 2023). Bulk instruments, such as gas chromatography, liquid chromatography, and gas or liquid chromatography-mass spectrometry, have the advantages of high precision, accuracy, and stability. However, these methods suffer from expensive equipment, cumbersome procedures, high costs, professional operations, and long detection periods (Chadha et al., 2022; Wang et al., 2021). Rapid detection methods, such as enzyme-linked immunosorbent assay (ELISA) and lateral flow tests (LFTs), have the main advantages of simple operation and good specificity (Hongsibsong et al., 2020). However, due to the complex food matrix, these methods have a relatively high false positive rate and lack of stability (Zheng et al., 2020). Besides, they are usually not sensitive enough to detect pesticide residues, such as chlorpyrifos with trace levels. As new emerging analytical methods, biosensors are becoming more and more specific and sensitive, making them a valuable addition to applications in various fields.

Due to their low background interference and sensitive signal output of relaxation time, magnetic relaxation switching (MRS) biosensors have been widely used in food safety detection and clinical diagnostics (Perez et al., 2002, 2004). Conventional MRS immunosensors rely on the state change of magnetic probes, which will affect the transverse relaxation time (T_2) of surrounding water molecules to realize the quantitative analysis of targets. However, conventional MRS immunosensors lack an effective signal amplification strategy and suffer from disadvantages, such as small relaxation signal variation and narrow detection range, due to the limited change in the state of magnetic probes, leading to unsatisfactory detection results and limiting their application in rapid food safety detection (Chen et al., 2018; Sun et al., 2006). In particular, chlorpyrifos is a small molecule that has only one binding site for the corresponding antibody, which cannot lead to an obvious change in T_2 signals, thus greatly limiting the sensitivity of MRS detection in food samples (Dong et al., 2021; Zheng et al., 2020). Therefore, conventional MRS immunosensors hard to satisfy the demands for the detection of trace chlorpyrifos. Effective signal amplification strategies may be a feasible way to solve this problem.

The enzymatic reaction-mediated tyramine signal amplification (TSA) system is an efficient signal amplification technique (Akama et al., 2016). In the presence of hydrogen peroxide (H_2O_2) and horseradish peroxidase (HRP), tyramine can be converted into a highly reactive intermediate that tends to covalently bind on nearby proteins (Cao et al., 2021; Hu et al., 2022; Yuan et al., 2012). Owing to the convenient operations and rapid detection, the TSA system was combined with the immunoassay to achieve sensitive and specific detection of various analytes. In the previous work (Chen et al., 2023), the TSA system has been used to develop a novel microparticle counting immunosensor. Tyramine-functionalized polystyrene microspheres (PS-tyramine) were used as the signal probes. The TSA system enables assembling PS-Tyramine with the magnetic carrier in the presence of HRP and H_2O_2. The unbound PS-tyramine probes were used for signal readout, which corresponds to the target concentration. The sensitivity of this microparticle-counting immunosensor has improved by 1–2 orders of magnitude than that of the ELISA method for the detection of aflatoxin B_1. Based on the imaging sensor array and TSA strategy, Zong et al. proposed a novel chemiluminescence (CL) immunosensor array for rapid and sensitive detection of mycotoxins in herbal medicine (Zong et al., 2021). Wherein, biotinylated tyramine was activated to be numerous radicals by HRP and then covalently coupled with streptavidin-HRP with the rapid growth of HRP on the "antibody–antigen" structure, resulting in effective signal amplification. This strategy showed excellent sensitivity, wide linear detection ranges, good stability and selectivity, and rapid and easy operation. These works prove that the TSA system can indeed improve the analytical performance of biosensors and can be used as a potential means to improve the performance of the conventional MRS immunosensor for the detection of trace small molecules.

In this work, by combining the TSA system with the MRS technique, we developed a TSA-MRS immunosensor for the rapid and sensitive detection of chlorpyrifos. In the TSA-MRS immunosensor, chlorpyrifos can regulate the loading amount of HRP via an immunoreaction between antigen and antibody. In the presence of HRP and H_2O_2, it will activate a large number of tyramines to form highly reactive intermediates, which in turn drive the combination of tyramine-modified magnetic probes with the nearby "HRP-antibody-magnetic particles", forming an aggregation of the magnetic particles (Scheme 1a). The state change causes a significant variation in the T_2 signal and reflects a correlation between chlorpyrifos and T_2 signal, allowing for quantitative detection of chlorpyrifos. Based on the competitive immunoassay, in the presence of chlorpyrifos, less HRP-Ab_2 will bind to the surface of the magnetic separation carrier, which in turn activates less tyramine, resulting in insignificant magnetic probe aggregation and weak T_2 signal changes (Scheme 1b). The TSA-MRS immunosensor can effectively improve the detection sensitivity and analytical efficiency and enhance the performance of MRS immunosensors for pesticide residue detection.

2 | MATERIALS AND METHODS

2.1 | Materials and instrumentation

Chlorpyrifos, N-hydroxysuccinimide (NHS), 1-ethyl-3 [3- dimethylaminopropyl] carbodiimide hydrochloride (EDC), acephate, triazophos, glyphosate, dimethoate, and tyramine were purchased from Shanghai
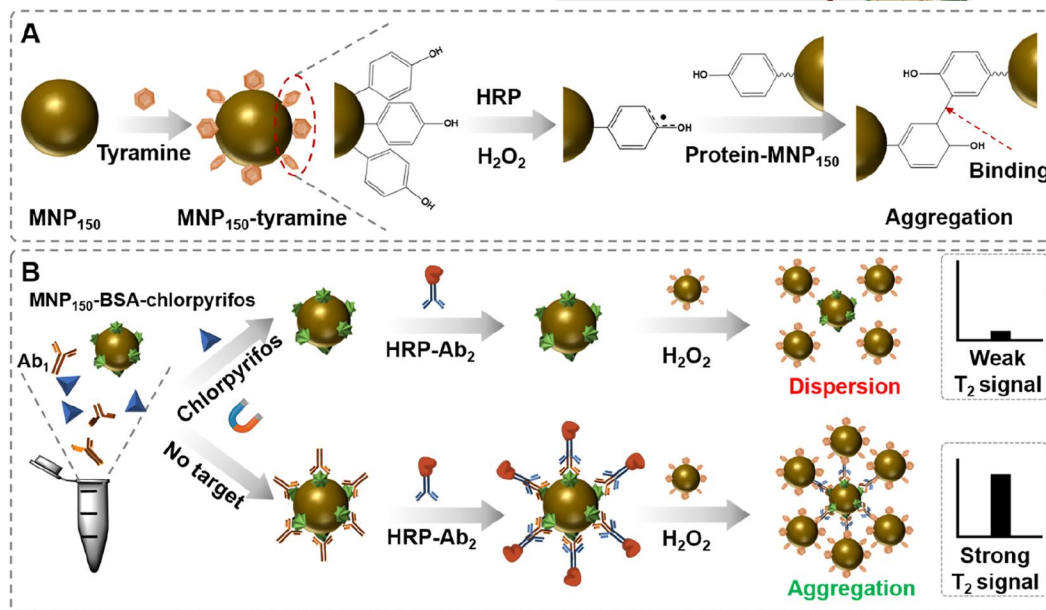
SCHEME 1 Schematic presentation of TSA-MRS immunosensor for the detection of chlorpyrifos. (a) Enzymatic tyramine-mediated magnetic nanoparticle aggregation strategy; (b) Competitive magnetic relaxation switching (MRS) immunoassay for chlorpyrifos.

Aladdin Biochemical Technology Co., Ltd. (Shanghai, China). Magnetic nanoparticles modified with carboxylic acid (COOH-MNP_{150}) with an average diameter of 150 nm (solid content: 10 mg/mL) were purchased from Ocean NanoTech (USA). Monoclonal antibody for chlorpyrifos (Ab_1) and complete antigen (BSA-chlorpyrifos) were purchased from Shan-dong Lvdu Bio-sciences & Technology Co., Ltd. (Shandong, China). Sheep anti-mouse secondary antibody (Ab_2) was purchased from Beijing Biodragon Immunotechnologies Co., Ltd. (Beijing, China). Other chemicals were analytical reagent grade from Sinopharm Chemical Reagent Co., Ltd. (Shanghai, China). Phosphate buffered saline (PBS, pH 7.4) and PBST (containing 0.05% Tween-20) were prepared in deionized water produced by the Millipore Milli-Q ion exchange apparatus.

0.47T NMR instrument (PQ001) (Shanghai Niu mag Corp.) was used to measure the T_2 values. The Nano ZS (Malvern Instruments Ltd. England) was used to analyze the hydrodynamic size and Zeta potential change of MNP_{150} and MNP_{150}-tyramine. Fourier Transform Infrared Spectrometer (FTIR) (IS50) (Suzhou Opus Plasma Technology Co., LTD) was used to characterize the MNP_{150} and MNP_{150}-tyramine. The field emission transmission electron microscope (TEM) (JEM-2100F, Japanese) was used to characterize the MNP_{150}-tyramine and magnetic nanoparticle clusters.

2.2 | Preparation of MNP_{150}-tyramine conjugate

An amount of 1 mg of COOH-MNP_{150} was mixed with EDC (10 mg/mL, 20 µL) and NHS (10 mg/mL, 10 µL) and slowly vortexed for 20 min at room temperature. After activation, magnetic separation was performed and resuspended in PBS buffer. An amount of 0.5 mg of tyramine was added and vortexed slowly for 2 h at room

temperature and overnight at 4°C. After completion of the reaction, the magnetic separation was washed twice with PBST. The MNP_{150}-tyramine conjugate was finally resuspended with 500 µL PBS buffer and stored at 4°C.

2.3 | Preparation of MNP_{150}-BSA-chlorpyrifos conjugate

An amount of 1 mg of COOH-MNP_{150} was mixed with EDC (10 mg/mL, 20 µL) and NHS (10 mg/mL, 10 µL) and slowly vortexed for 20 min at room temperature. After activation, magnetic separation was performed and resuspended with PBS buffer. An amount of 40 µg BSA-chlorpyrifos was added and slowly vortexed for 2 h at room temperature. After completion of the reaction, 500 µL BSA (3%) was added and closed for 30 min. Then, magnetic separation was performed and washed 3 times with PBST. The MNP_{150}-BSA-chlorpyrifos conjugate was finally resuspended with 1000 µL PBS buffer and stored at 4°C.

2.4 | Detection of chlorpyrifos by the enzymatic tyramine-MRS immunosensor

An amount of 100 µL of graded concentrations of the chlorpyrifos solution (0, 1, 5, 10, 50, 100, 500, and 1000 ng/mL) was mixed with 50 µL of Ab (2.6 µg/mL) solution and slowly vortexed for 15 min. Then, 50 µL MNP_{150}-BSA-chlorpyrifos (100 µg/mL) was added, and the competitive immune reaction was carried out at 37°C for 20 min. After magnetic separation, washing, and resuspension, 100 µL Ab_2 (diluted 500-fold) was added and the reaction was carried out at

37°C for 20 min. After magnetic separation and washing 3 times with PBST, the conjugates was resuspended with 150 µL of PBS buffer. An amount of 50 µL MNP_{150}-tyramine (5 µg/mL with 5% H_2O_2) was added and the reaction was carried out for 10 min at room temperature. After the reaction was completed, the reaction solution was added to 800 µL of pure water and the T_2 values were determined. T_2 measurements were performed using a CPMG pulse sequence with the following parameters: NMR frequency of 19.894 MHz, TW (ms) of 18,000, TE (ms) of 1, PRG of 3, NECH of 18,000, and SW of 100.

2.5 | Detection of chlorpyrifos in orange samples

The oranges were bought in the local supermarket and cut into small pieces and homogenized, then accurately weighed into the test tube and 10 mL acetonitrile was added. Next, the samples were vibrated at a high speed for 2 min and filtered using filter paper. The filtrate was collected and 1.2 g sodium chloride was added, violently extracted for 1 min, and kept at room temperature for 30 min. Finally, the filtrate was filtered by the 0.22 µm filter membrane and diluted by PBS. The detected concentration of chlorpyrifos in samples was calculated according to the standard regression equation. The results were verified and compared with gas chromatography (SN/T 2158-2008).

3 | RESULTS AND DISCUSSION

3.1 | Principles of TSA-MRS immunosensor

The main principle of TSA is to use the peroxidase reaction of tyramide (tyramide salt forms a covalent bond binding site under HRP catalysis of H_2O_2) to produce a large number of enzymatic products, which can bind with the surrounding protein residues so that a large number of labels are deposited at the antigen–antibody binding site (Scheme 2). When chlorpyrifos exists in the samples, it will be able to compete with BSA-chlorpyrifos on MNP_{150} and bind with Ab_1. A higher level of chlorpyrifos will lead to less Ab_1 bound to MNP_{150}-BSA-chlorpyrifos and further fewer combinations of Ab_1 and Ab_2-HRP. As such, the MNP_{150}-BSA-chlorpyrifos complex is in a dispersed state with weaker changes in T_2 values. Conversely, MNP_{150}-tyramine will combine with MNP_{150}-BSA-chlorpyrifos with an aggregated state, showing stronger changes in T_2 values.

3.2 | Characterization of MNP_{150}-tyramine

MNP_{150}-tyramine was characterized by dynamic light scattering and Fourier transform infrared spectroscopy (FT-IR). After tyramine modification, the hydration particle size of MNP_{150} increases from 203 to 288 nm (Figure 1a), and the Zeta potential changes from −28.7 mV to −34.7 mV (Figure 1b), which is caused by the increase of negative charge on the surface of MNP_{150}. The infrared spectrum of tyramine showed several characteristic peaks, among which the benzene carbon skeleton stretching vibration peak is shown at 1594 cm^{-1}, 1516 cm^{-1}, and 1379 cm^{-1}. N-H symmetric and anti-symmetric stretching vibration peaks are shown at 3335 cm^{-1} and 3282 cm^{-1}. After the modification of tyramine, MNP_{150} has a larger peak at 3448 cm^{-1} and a new absorption peak at 1648 cm^{-1} (Figure 1c), which is presumed to be the amide bond formed by the modification of tyramine. These results indicated that tyramine was successfully modified on the surface of MNP_{150}.

### 3.3 | Enzymatic tyramine-MRS signal readout system

Based on the tyramine signal amplification technique, we constructed an enzymatic tyramine-MRS signal readout system. The change in the state of the magnetic particles before and after the formation of aggregates was observed by TEM images. As shown in Figure 2a, prior to the reaction, MNP_{150}-tyramine was in a dispersed state. After MNP_{150} aggregation was induced by immunoreaction and enzymatic-tyramine reaction, the magnetic particle cluster was formed with a clearly aggregated state (Figure 2b).

This signal readout system was further validated by the measurement of T_2 values. As depicted in Figure 2c, T_2 signal change (ΔT_2) was the most significant for MNP_{150} complexes. Whereas, when only Ab_2-HRP was present, a weaker T_2 signal change was produced due to a weak aggregation state caused by collisions generated by the tyramine oxidation intermediate-MNP_{150} catalyzed by HRP. In the absence of HRP or H_2O_2, tyramine could not be converted to highly reactive oxidation intermediates and therefore could not cause aggregation of magnetic particles and changes in the T_2 signal. In contrast, there is no significant ΔT_2 in the absence of Ab_1 due to the washing process, resulting in the absence of HRP in the final reaction system. Furthermore, the hydrated particle size of MNP_{150}-BSA-chlorpyrifos increased significantly after the formation of magnetic particle clusters (Figure 2d). Therefore, the TSA system is well feasible for the subsequent construction of TSA-MRS immunosensors.

3.4 | Optimization for TSA-MRS immunosensor

To improve the analytical performance of the TSA-MRS immunosensor, the addition concentration of H_2O_2 was first optimized. As shown in Figure 3a, ΔT_2 values were the highest when the H_2O_2 concentration was 5%, that is, 5% H_2O_2 had the greatest change in T_2 values, whereas when the H_2O_2 concentration is lower than 5%, the T_2 signal response is weak because the initial radical produced by H_2O_2 is insufficient to induce the TSA reaction. When the H_2O_2 concentration was higher than 5%, the ΔT_2 value decreased slightly and may be ascribed to the unstable enzymatic reaction at a high concentration of H_2O_2. Therefore, 5% H_2O_2 was selected for the optimal condition in the following experiments.

SCHEME 2 Principle of the tyramine signal amplification (TSA) strategy in the construction of the magnetic relaxation switching (MRS) immunosensor from a dispersive state to an aggregated state.
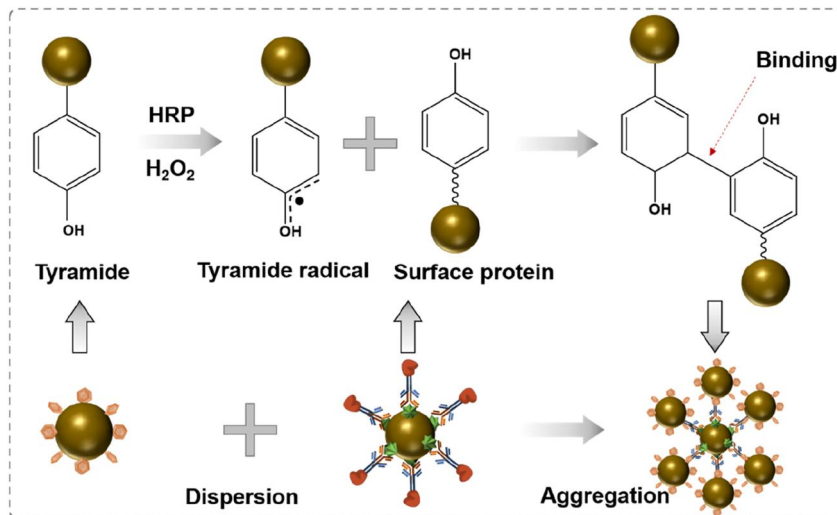

FIGURE 1 Characterization of MNP$_{150}$-tyramine. (a) Hydrodynamic size, (b) Zeta potential, and (c) FT-IR spectra of MNP$_{150}$ and MNP$_{150}$-tyramine.
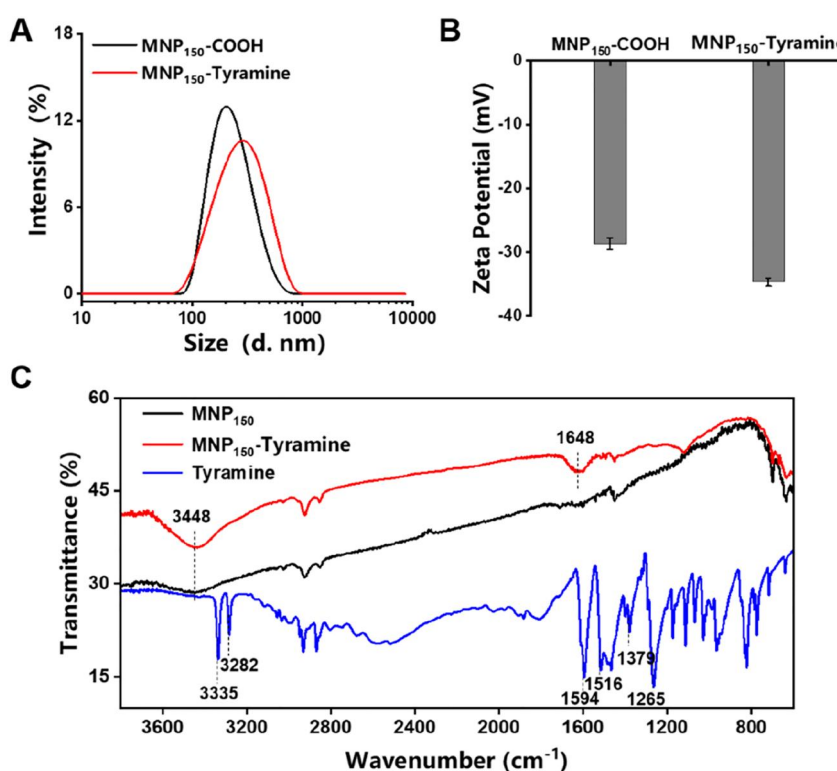
After that, the reaction time for TSA-induced magnetic particle aggregation was optimized (Figure 3b). After 10 min of reaction, ΔT_2 values increased slowly and tended to be balanced, which can be attributed to the magnetic particle aggregation state, had reached a near-saturation level and would not enhance significantly; therefore, it could not cause a significant increase in ΔT_2 values. As a result, 10 min was chosen as the optimal reaction time. Besides, the concentration of MNP$_{150}$-tyramine was discussed. The TSA-MRS immunosensor showed the highest signal response to chlorpyrifos when the concentration of MNP$_{150}$-tyramine was 5 μg/mL (Figure 3c). In contrast, when the MNP$_{150}$-tyramine concentration was 2 μg/mL, the response was lower due to the low concentration of the magnetic probe and insufficient aggregation state. When the concentration of MNP$_{150}$-tyramine was 10 μg/mL, the magnetic probe concentration was high, the magnetic signal was too strong, and T$_2$ values changed a little, resulting in weak ΔT_2 values. Therefore, the best concentration of MNP$_{150}$-tyramine was selected as 5 μg/mL.

As exhibited in Figure 3d, the concentration of MNP$_{150}$-BSA-chlorpyrifos in the immunoreaction process was explored. When its concentration was 50 μg/mL, the TSA-MRS immunosensor response tended to flatten out when chlorpyrifos is at high concentrations, indicating that the concentration of MNP$_{150}$-BSA-chlorpyrifos was insufficient during the immunoreaction process. However, when the
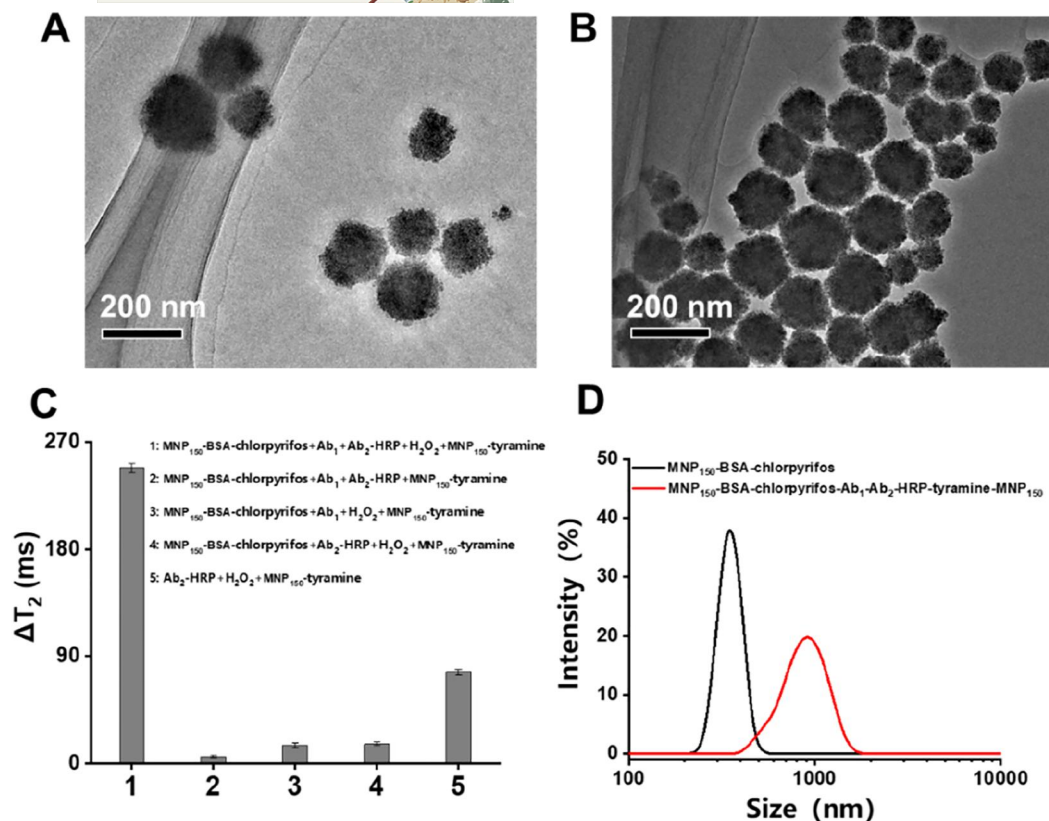
FIGURE 2 Feasibility validation of the enzymatic tyramine-mediated magnetic relaxation switching (MRS) signal readout system. (a) TEM images of MNP_{150}-tyramine and (b) magnetic nanoparticle clusters; (c) Magnetic signal changes of TSA-MRS sensing before and after the reaction; and (d) Hydrodynamic size of MNP_{150}-BSA-chlorpyrifos and magnetic nanoparticle clusters.

concentration of MNP_{150}-BSA-chlorpyrifos is higher (200 µg/mL), the magnetic signal tended to be weak, and the ΔT_2 value was close to 0 when chlorpyrifos is at a low concentration, which was not favorable for the detection of low concentrations of chlorpyrifos. Thus, 100 µg/mL of MNP_{150}-BSA-chlorpyrifos was chosen for subsequent experiments.

Obviously, the concentration of MNP_{150}-BSA-chlorpyrifos is greater than that of MNP_{150}-tyramine. In the TSA-MRS sensing system, MNP_{150}-tyramine acts as a promoter for magnetic particle aggregation and MNP_{150}-tyramine contains a large amount of tyramine on its surface. When the concentration of MNP_{150}-tyramine is too high, excess MNP_{150}-tyramine will remain in the solution and lead to a weak ΔT_2 value.

3.5 | TSA-MRS immunosensor for the detection of chlorpyrifos

The sensitivity of the TSA-MRS immunosensor was investigated under the above optimal conditions. As displayed in Figure 4a, the ΔT_2 value for chlorpyrifos increased gradually over the concentration ranging from 1 ng/mL to 1000 ng/mL. The TSA-MRS immunosensor showed a wide linear range from 1 to 100 ng/mL with a regression equation of $Y = 90.39 X + 11.66$, ($X = $ Lg[chlorpyrifos]

and $R^2 = 0.99$) and a limit of detection (LOD) of 0.54 ng/mL (LOD $= 3S/M$, $S = 2.74$, and $M = 15.24$) (Figure 4b). The sensitivity of the conventional ELISA method for chlorpyrifos was also analyzed and compared with the TSA-MRS method (Figure 4c). The linear range of the conventional ELISA for chlorpyrifos was 5~100 ng/mL with a linear regression equation of $Y = 0.61 X + 0.02$, ($X = $ Lg[chlorpyrifos] and $R^2 = 0.99$) and a limit of detection of 2.43 ng/mL ($S = 0.038$, $M = 0.047$) (Figure 4d). In comparison, the sensitivity of TSA-MRS immunosensor was 4.5-fold higher than that of the conventional ELISA method with a linear range skewed toward lower concentrations and better analytical performance. In addition, this TSA-MRS immunosensor has lower cost, less reagent consumption, fewer operating steps, and shorter detection time than the conventional ELISA method for chlorpyrifos (Table S1).

The superior analytical performance of the TSA-MRS immunosensor can be attributed to the following factors: (1) the HRP-catalyzed tyramine signal amplification system effectively changes the state of magnetic particles, thus significantly increasing the value of the magnetic signal change. (2) The large specific surface area of magnetic particles at the nanoscale level allows for the coupling of large amounts of tyramine or antibodies, which increased the efficiency of the TSA reaction. As a result, the TSA-MRS immunosensor outcompetes the ELISA method in detection sensitivity.
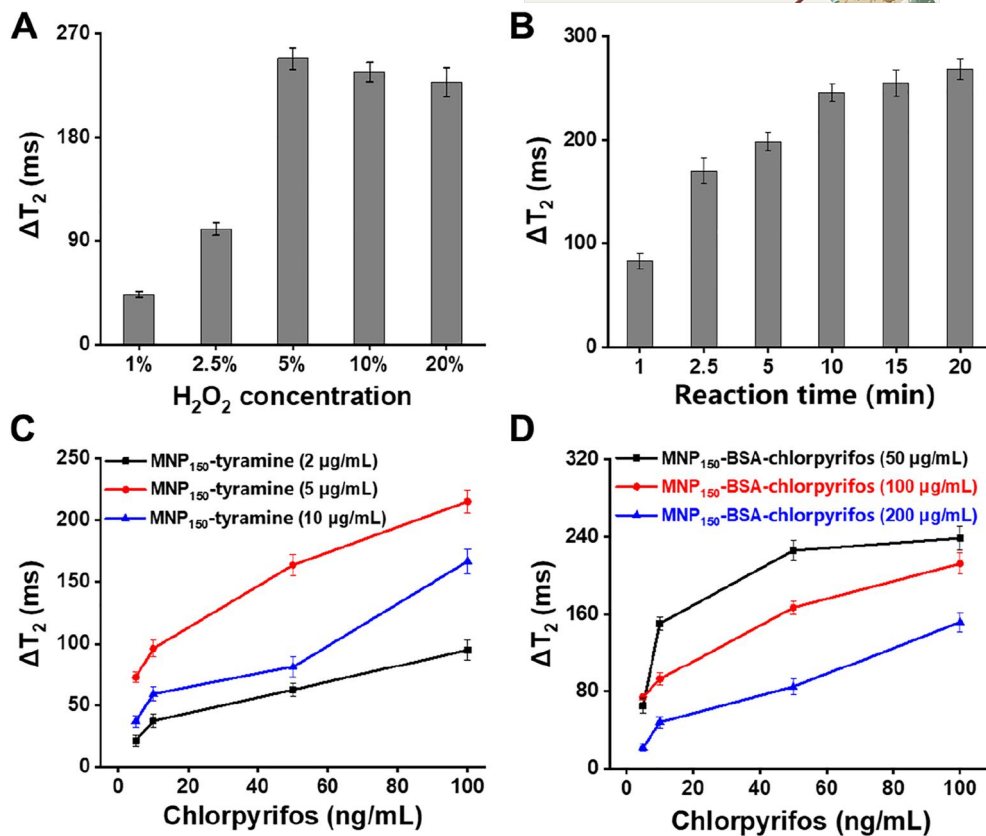
FIGURE 3 Optimization of TSA-MRS immunosensor for the detection of chlorpyrifos. (a) H_2O_2 concentration; (b) reaction time of TSA-mediated aggregation of magnetic nanoparticle; (c) concentration of MNP_{150}-tyramine; and (d) MNP_{150}-BSA-chlorpyrifos.
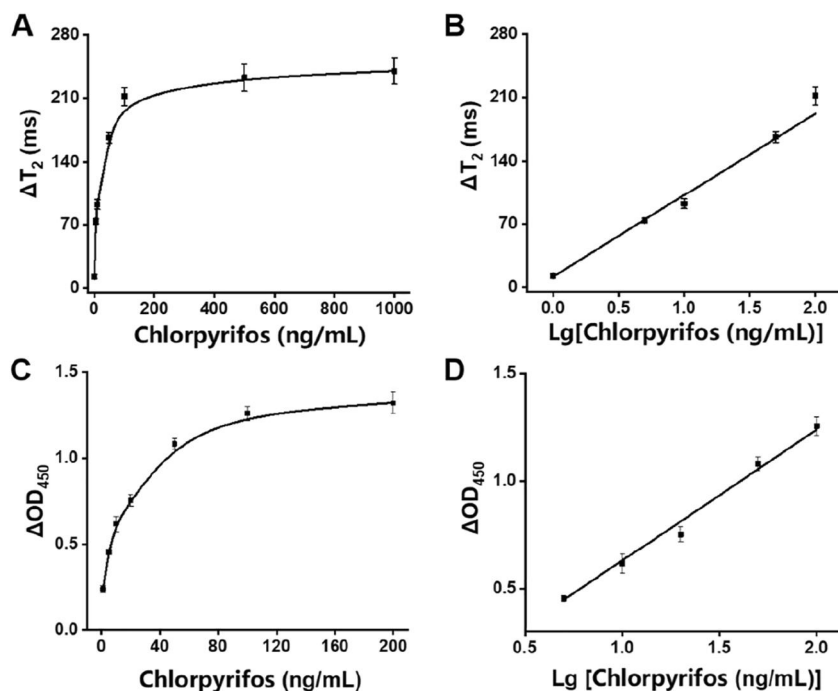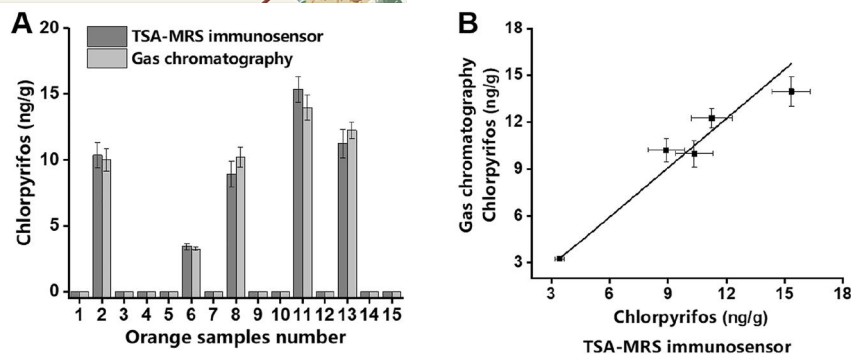

FIGURE 4 Detection results of TSA-MRS immunosensor and ELISA for chlorpyrifos. (a) Plots of ΔT_2 signal and (b) linear range of TSA-MRS immunosensor for the detection of chlorpyrifos. (c) Plots of ΔOD_{450} value and (d) linear range of ELISA for the detection of chlorpyrifos.

FIGURE 5 Detection of chlorpyrifos in orange samples using the TSA-MRS immunosensor. (a) Comparison of TSA-MRS immunosensor and gas chromatography for the detection of chlorpyrifos in orange samples. (b) Correlation between TSA-MRS immunosensor and gas chromatography for the detection of chlorpyrifos in orange samples.

3.6 | Selectivity and reproducibility of enzymatic tyramine-MRS immunosensor

The specificity of the TSA-MRS immunosensor for chlorpyrifos was evaluated using chlorpyrifos analogs or pesticides that are usually simultaneously applied in fruits and vegetables (Figure S1a), including glyphosate, triazophos, acephate, parathion, dimethoate, dichlorvos, and chlorthion. As shown in Figure S1b, only chlorpyrifos was able to induce significant changes in T_2 values, while the other interferents produced only weak changes in the T_2 signal even at 10 times the concentration of chlorpyrifos, indicating that the TSA-MRS immunosensor possessed good specificity in detecting chlorpyrifos due to the high selectivity of the immune response.

In addition, the recoveries of chlorpyrifos detected by the TSA-MRS immunosensor were determined by adding 10–80 ng/mL of chlorpyrifos to blank orange samples (Table S2). The results showed that the recoveries of chlorpyrifos ranged from 73.63% to 86.17% with coefficients of variation of 9.97%–14.42%, indicating that the method has an acceptable accuracy in detecting chlorpyrifos.

3.7 | Detection of chlorpyrifos poisoning in orange samples

Oranges, one of the most produced fruits in China, are often used to control pests and increase yields through the use of pesticides such as chlorpyrifos. Therefore, in this study, oranges were selected as the samples to be detected. 15 orange samples were purchased from local supermarkets for assessing the capability of TSA-MRS immunosensor in actual sample detection. The results of chlorpyrifos content determination were compared with gas chromatography to determine the accuracy of the TSA-MRS immunosensor. As shown in Figure 5a, samples 2, 6, 8, 11, and 13 were detected as positive, but all were below the maximum detectable limit (1 mg/kg) (GB 2763-2021). Moreover, the detection results of the TSA-MRS immunosensor agreed well with the gas chromatography method (Figure 5b).

The results demonstrated that the constructed TSA-MRS immunosensor showed good detection capability for real samples. Compared with the gas chromatography method, our TSA-MRS immunosensor is low cost, high efficiency, and requires no specialized skills and expensive instruments. We also summarized and compared the previous works for the detection of chlorpyrifos with our assay (Table S3). Our TSA-MRS immunosensor has a higher sensitivity and a broader linear range than traditional or other reported assays, providing a potential method for harmful substances in resource-constrained areas.

4 | CONCLUSION

Overall, a novel TSA-MRS immunosensor was developed for the rapid and sensitive detection of chlorpyrifos. In the study, MNP_{150}-BSA-chlorpyrifos acts as an antigen substrate for specific antibody recognition and magnetic separation, MNP_{150}-tyramine as magnetic probes for signal readout, and TSA strategy for signal amplification. The TSA-MRS immunosensor showed good analytical performance toward chlorpyrifos with a wide linear response from 1 to 100 ng/mL ($R^2 = 0.99$), a low LOD of 0.54 ng/mL, and acceptable recoveries of 73.63%–86.17% in orange samples. The method can be used for the rapid detection of other food contaminants by simply replacing antibodies corresponding to the target, providing a simple and easy-to-use idea for rapid food safety detection. In the future, it will be closer to practical applications by combining automated equipment to enable the simultaneous detection of multiple pesticide residue targets.

AUTHOR CONTRIBUTIONS
Chen Zhan: Data curation; investigation; methodology; software; writing – original draft. **Long Wu**: Funding acquisition; project administration; resources; supervision; writing – review and editing. **Yongzhen Dong**: Conceptualization; formal analysis; methodology; validation; visualization; writing – review and editing.

CONFLICT OF INTEREST STATEMENT

We wish to draw the attention of the Editor to the following facts which may be considered as potential conflicts of interest and to significant financial contributions to this work. We wish to confirm that there are no known conflicts of interest associated with this publication and there has been no significant financial support for this work that could have influenced its outcome. We confirm that the manuscript has been read and approved by all named authors and that there are no other persons who satisfied the criteria for authorship but are not listed. We further confirm that the order of authors listed in the manuscript has been approved by all of us. The authors declare no conflict of interest.

DATA AVAILABILITY STATEMENT

The data that support the findings of this study are available in the supplementary material of this article.

ETHICS STATEMENT

None declared.

ORCID

Yongzhen Dong https://orcid.org/0000-0002-5394-9418

REFERENCES

Akama, K., Shirai, K., & Suzuki, S. (2016). Droplet-free digital enzyme-linked immunosorbent assay based on a tyramide signal amplification system. *Analytical Chemistry*, 88(14), 7123–7129. https://doi.org/10.1021/acs.analchem.6b01148

Cao, J. T., Zhao, L. Z., Fu, Y. Z., Liu, X. M., Ren, S. W., & Liu, Y. M. (2021). Tyramide signal amplification and enzyme biocatalytic precipitation on closed bipolar electrode: Toward highly sensitive electrochemiluminescence immunoassay. *Sensors and Actuators, A: Chemical*, 331, 129427. https://doi.org/10.1016/j.snb.2020.129427

Chadha, R., Das, A., Lobo, J., Meenu, V. O., Paul, A., Ballal, A., & Maiti, N. (2022). γ-Cyclodextrin capped silver and gold nanoparticles as colorimetric and Raman sensor for detecting traces of pesticide "Chlorpyrifos" in fruits and vegetables. *Colloids and Surfaces, A: Physicochemical and Engineering Aspects*, 641, 128558. https://doi.org/10.1016/j.colsurfa.2022.128558

Chen, R., Zhan, C., Huang, C., He, Q., Bao, J., Zhang, X., Pi, Z., & Chen, Y. (2023). Tyramine signal amplification on polystyrene microspheres for highly sensitive quantification of Aflatoxin B1 in peanut samples. *Sensors and Actuators B: Chemical*, 378.

Chen, Y. P., Yin, B. F., Dong, M. L., Xianyu, Y. L., & Jiang, X. Y. (2018). Versatile T_1-based chemical analysis platform using Fe^{3+}/Fe^{2+} interconversion. *Analytical Chemistry*, 90(2), 1234–1240. https://doi.org/10.1021/acs.analchem.7b03961

Dong, S., Shi, Q. Y., He, K. L., Wu, J. W., Zhu, Z. X., & Feng, J. G. (2022). A simple aptamer SERS sensor based on mesoporous silica for the detection of chlorpyrifos. *Foods*, 11(21), 3331. https://doi.org/10.3390/foods11213331

Dong, Y. Z., Wen, C. Y., She, Y. X., Zhang, Y., Chen, Y. P., & Zeng, J. B. (2021). Magnetic relaxation switching immunoassay based on hydrogen peroxide-mediated assembly of Ag@Au-Fe₃O₄ nanoprobe for detection of aflatoxin B1. *Small*, 17(51), e2104596. https://doi.org/10.1002/smll.202104596

Gosset, A., Polome, P., & Perrodin, Y. (2020). Ecotoxicological risk assessment of micropollutants from treated urban wastewater effluents for watercourses at a territorial scale: Application and comparison of two approaches. *International Journal of Hygiene and Environmental Health*, 224, 113437. https://doi.org/10.1016/j.ijheh.2019.113437

Hongsibsong, S., Prapamontol, T., Xu, T., Hammock, B. D., Wang, H., Chen, Z. J., & Xu, Z. L. (2020). Monitoring of the organophosphate pesticide chlorpyrifos in vegetable samples from local markets in northern Thailand by developed immunoassay. *International Journal of Environmental Research and Public Health*, 17(13), 4723. https://doi.org/10.3390/ijerph17134723

Hou, J., Zhang, F., Wang, P. F., Wang, C., Chen, J., Xu, Y., You, G. X., Zhou, Q., & Li, Z. Y. (2018). Enhanced anaerobic biological treatment of chlorpyrifos in farmland drainage with zero valent iron. *Chemical Engineering Journal*, 336, 352–360. https://doi.org/10.1016/j.cej.2017.12.032

Hu, T., Ke, X., Ou, Y., & Lin, Y. (2022). CRISPR/Cas12a-Triggered chemiluminescence enhancement biosensor for sensitive detection of nucleic acids by introducing a tyramide signal amplification strategy. *Analytical Chemistry*, 94(23), 8506–8513. https://doi.org/10.1021/acs.analchem.2c01507

Katsikantami, I., Colosio, C., Alegakis, A., Tzatzarakis, M. N., Vakonaki, E., Rizos, A. K., Sarigiannis, D. A., & Tsatsakis, A. M. (2019). Estimation of daily intake and risk assessment of organophosphorus pesticides based on biomonitoring data - the internal exposure approach. *Food and Chemical Toxicology*, 123, 57–71. https://doi.org/10.1016/j.fct.2018.10.047

Khalid, S., Shahid, M., Murtaza, B., Bibi, I., Natasha, Asif Naeem, M., & Niazi, N. K. (2020). A critical review of different factors governing the fate of pesticides in soil under biochar application. *Science of the Total Environment*, 711, 134645. https://doi.org/10.1016/j.scitotenv.2019.134645

Li, T. S., Wang, J., Zhu, L. J., Li, C. W., Chang, Q. Y., & Xu, W. T. (2022). Advanced screening and tailoring strategies of pesticide aptamer for constructing biosensor. *Critical Reviews in Food Science and Nutrition*, 1–21. https://doi.org/10.1080/10408398.2022.2086210

Liu, T., Xu, S. R., Lu, S. Y., Qin, P., Bi, B., Ding, H. D., Liu, Y., Guo, X. C., & Liu, X. H. (2019). A review on removal of organophosphorus pesticides in constructed wetland: Performance, mechanism and influencing factors. *Science of the Total Environment*, 651, 2247–2268. https://doi.org/10.1016/j.scitotenv.2018.10.087

Mie, A., Ruden, C., & Grandjean, P. (2018). Safety of safety evaluation of pesticides: Developmental neurotoxicity of chlorpyrifos and chlorpyrifos-methyl. *Environmental Health*, 17(1), 77. https://doi.org/10.1186/s12940-018-0421-y

Perez, J. M., Josephson, L., Loughlin, T. O., Hogemann, D., & Weissleder, R. (2002). Magnetic relaxation switches capable of sensing molecular interactions. *Nature Biotechnology*, 20(8), 816–820. https://doi.org/10.1038/nbt720

Perez, J. M., Josephson, L., & Weissleder, R. (2004). Use of magnetic nanoparticles as nanosensors to probe for molecular interactions. *ChemBioChem*, 5(3), 261–264. https://doi.org/10.1002/cbic.200300730

Pundir, C. S., Malik, A., & Preety (2019). Bio-sensing of organophosphorus pesticides: A review. *Biosensors & Bioelectronics*, 140, 111348. https://doi.org/10.1016/j.bios.2019.111348

Samsidar, A., Siddiquee, S., & Shaarani, S. M. (2018). A review of extraction, analytical and advanced methods for determination of pesticides in environment and foodstuffs. *Trends in Food Science & Technology*, 71, 188–201. https://doi.org/10.1016/j.tifs.2017.11.011

Sun, E. Y., Weissleder, R., & Josephson, L. (2006). Continuous analyte sensing with magnetic nanoswitches. *Small*, *2*(10), 1144–1147. https://doi.org/10.1002/smll.200600204

Theansun, W., Sriprachuabwong, C., Chuenchom, L., Prajongtat, P., Techasakul, S., Tuantranont, A., & Dechtrirat, D. (2023). Acetylcholinesterase modified inkjet-printed graphene/gold nanoparticle/poly (3,4-ethylenedioxythiophene):poly(styrenesulfonate) hybrid electrode for ultrasensitive chlorpyrifos detection. *Bioelectrochemistry*, *149*, 108305. https://doi.org/10.1016/j.bioelechem.2022.108305

Wang, H. X., Liang, D., Xu, Y., Liang, X., Qiu, X. Q., & Lin, Z. (2021). A highly efficient photoelectrochemical sensor for detection of chlorpyrifos based on 2D/2D β-Bi_2O_3/g-C_3N_4 heterojunctions. *Environmental Science: Nano*, *8*(3), 773–783. https://doi.org/10.1039/d0en01243b

Xu, M. L., Gao, Y., Han, X. X., & Zhao, B. (2017). Detection of pesticide residues in food using surface-enhanced Raman spectroscopy: A review. *Journal of Agricultural and Food Chemistry*, *65*(32), 6719–6726. https://doi.org/10.1021/acs.jafc.7b02504

Yuan, L., Xu, L. L., & Liu, S. Q. (2012). Integrated tyramide and polymerization-assisted signal amplification for a highly-sensitive immunoassay. *Analytical Chemistry*, *84*(24), 10737–10744. https://doi.org/10.1021/ac302439v

Zhang, L. X., Feng, L. P., Jiang, J. T., Li, P., Chen, X., Zhang, S., Gao, Y., Hong, R. X., Chen, G. F., Mao, G. J., & Wang, H. (2021). A highly sensitive and visible-light-driven photoelectrochemical sensor for chlorpyrifos detection using hollow Co_9S_8@CdS heterostructures. *Sensors and Actuators, B: Chemical*, *348*, 130719. https://doi.org/10.1016/j.snb.2021.130719

Zheng, W. S., Zeng, L. W., & Chen, Y. P. (2020). Bioorthogonal reactions amplify magnetic nanoparticles binding and assembly for ultrasensitive magnetic resonance sensing. *Analytical Chemistry*, *92*(3), 2787–2793. https://doi.org/10.1021/acs.analchem.9b05097

Zhu, Q., Cao, W., Gao, H., Chen, N., Wang, B. N., & Yu, S. F. (2010). Effects of the processing steps on chlorpyrifos levels during honey production. *Food Control*, *21*(11), 1497–1499. https://doi.org/10.1016/j.foodcont.2010.04.022

Zong, C., Jiang, F., Wang, X., Li, P., Xu, L., & Yang, H. (2021). Imaging sensor array coupled with dual-signal amplification strategy for ultrasensitive chemiluminescence immunoassay of multiple mycotoxins. *Biosensors & Bioelectronics*, *177*, 112998. https://doi.org/10.1016/j.bios.2021.112998

SUPPORTING INFORMATION

Additional supporting information can be found online in the Supporting Information section at the end of this article.